High Efficiency Uniform Wakefield Acceleration of a Positron Beam Using Stable Asymmetric Mode in a Hollow Channel Plasma

Shiyu Zhou,[1] Jianfei Hua[ORCID],[1] Weiming An,[2] Warren B. Mori,[3] Chan Joshi,[3] Jie Gao,[5] and Wei Lu[1,4,*]

[1]*Department of Engineering Physics, Tsinghua University, Beijing 100084, China*
[2]*Beijing Normal University, Beijing 100875, China*
[3]*University of California Los Angeles, Los Angeles, California 90095, USA*
[4]*Beijing Academy of Quantum Information Sciences, Beijing 100193, China*
[5]*Institute of High Energy Physics, Chinese Academy of Sciences, Beijing 100049, China*

Plasma wakefield acceleration in the blowout regime is particularly promising for high-energy acceleration of electron beams because of its potential to simultaneously provide large acceleration gradients and high energy transfer efficiency while maintaining excellent beam quality. However, no equivalent regime for positron acceleration in plasma wakes has been discovered to date. We show that after a short propagation distance, an asymmetric electron beam drives a stable wakefield in a hollow plasma channel that can be both accelerating and focusing for a positron beam. A high charge positron bunch placed at a suitable distance behind the drive bunch can beam-load or flatten the longitudinal wakefield and enhance the transverse focusing force, leading to high efficiency and narrow energy spread acceleration of the positrons. Three-dimensional quasistatic particle-in-cell simulations show that an over 30% energy extraction efficiency from the wake to the positrons and a 1% level energy spread can be simultaneously obtained. Further optimization is feasible.

High-energy electron-positron (e^-e^+) colliders are highly desirable for precision studies of the Higgs Boson and discovering physics beyond the standard model [1,2]. With the limitation on accelerating gradients imposed by breakdowns at tens of MV/m, current radio-frequency accelerators are close to the maximum cost and size limit of such colliders operating at the energy frontier of particle physics. This has spurred intense research on novel acceleration schemes with much higher acceleration gradients and wall plug efficiency. One promising candidate is plasma wakefield acceleration (PWFA) driven by a charge particle bunch [3–5]. PWFA has not only demonstrated accelerating gradients of tens of GV/m but also acceleration of a narrow energy spread e^- bunch with high efficiency [6,7]. In PWFA, the relativistic drive bunch can be electrons, positrons, or protons [8–12]. Most groundbreaking results to date have been obtained using an intense e^- bunch to excite a nonlinear wake that accelerates a second e^- bunch. However, this approach is not effective for e^+ acceleration because the volume at the very back of such wakes, where the wakefield is both accelerating and focusing for e^+, is extremely small. Various methods have been proposed to overcome this limitation. Because of the uniform accelerating field in transverse planes and zero focusing force inside channels, wakes in hollow plasma channels produced by more easily available e^- beams have been suggested for e^+ acceleration [13–17]. However, any misalignment of the drive and/or

trailing bunches induces a strong beam-breakup instability that leads to beam emittance growth and ultimately loss of positrons. This has limited further work on hollow channels for accelerating e^+ to high energy [18]. Recently, a hollow e^- beam was proposed for e^+ acceleration in a uniform plasma that creates a thin filament of plasma electrons on the axis that can focus and accelerate e^+ simultaneously. Its energy transfer efficiency is very limited, however, and it might be prone to kinetic instabilities [19]. In another proposal, a wake excited by an e^- beam in a finite-radius plasma column was proposed for e^+ transport and acceleration [20], where a narrow plasma electron filament is formed after the first wake cavity. However, the amount of accelerated charge seems very limited. In this Letter, we propose a nonlinear scheme that provides field structures suitable for stably accelerating and focusing a positron bunch inside a hollow plasma channel. In this scheme, the focusing field varies nearly linearly and the longitudinal field is almost independent of the transverse dimension throughout the channel in the region where the e^+ beam is placed. Such a field structure enables guided propagation and acceleration of a high charge e^+ beam. Furthermore, the e^+ beam efficiently loads the wake and gains energy while maintaining a narrow energy spread.

We first summarize how our scheme works. The trick is to excite a quadrupole transverse wakefield in the hollow plasma waveguide using an asymmetric ($\sigma_x \neq \sigma_y$) electron beam driver. Here, $\sigma_{x,y}$ are the beam rms spot sizes in
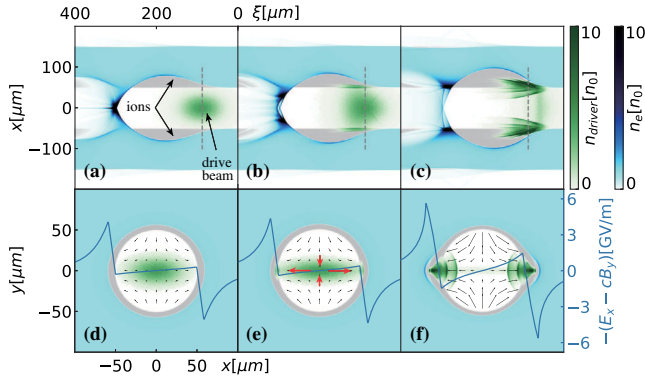
FIG. 1. Evolution of an asymmetric electron beam and wakefields in a hollow plasma channel. (a)–(c) Plasma and beam densities in $x - \xi$ plane (beam moves from left to right), and (d)–(f) at the cross section of beam center slice denoted by the gray dash line and transverse wakefields. Black arrows are the vector flow of transverse wakefield $-\vec{W}_\perp = -(E_x - cB_y)\hat{x} - (E_y + cB_x)\hat{y}$. Blue line is the lineout of $-\vec{W}_\perp$ at $y = 0$. Red arrows indicate the spot size evolution of the drive beam. The propagation distances are 0, 2.5, 10 cm from left to right.

transverse directions. As the beam propagates into the channel, its spot size evolution is determined by self-excited quadrupole wakefields, as shown in Fig. 1. The narrow part of the beam is focused, while the wider part is defocused until most electrons reach the inner plasma channel boundary in this plane. In the other plane, the electrons are tightly focused. A dense drive bunch will repel the plasma electrons from the wall while leaving behind the much more massive ions. Once this state is reached, the electron beam propagates with little further evolution because the defocusing quadrupole fields are balanced by focusing forces from the exposed ions. These ions subsequently pull back the plasma electrons forming a sheath [21]. This process is analogous to formation of a half-bubble on opposite sides of the channel wall except that the returning sheath electrons overshoot the initial channel boundary and fill the entire cross section of the hollow channel, providing a focusing force that guides the trailing e^+ bunch in both planes if it is placed in this region. This e^+ bunch can extract a considerable amount of energy by flattening or beam-loading the longitudinal accelerating field. Some plasma electrons are attracted toward the axis by the positrons and form a denser electron filament that enhances the focusing force. We will give a conceptual framework based on theory and then demonstrate it by 3D QuickPic [22,23] simulations.

Consider an ionized hollow plasma channel with density $n_p(r) = n_0 H(r - r_0)$, where H is the step function, r_0 is the channel radius, and n_0 is density of electrons. The wakefields driven by a relativistic point charge can be decomposed into discrete azimuthal modes [15]. For a bunch of drive particles, we rearrange the transverse wake functions by moments of beam position:

$$\vec{W}_{\perp 0}(x, y, \xi) = 0 \tag{1}$$

$$\vec{W}_{\perp 1}(x, y, \xi) = \lambda \hat{W}_{\perp 1}(\xi)[\langle x \rangle \hat{x} + \langle y \rangle \hat{y}] \tag{2}$$

$$\vec{W}_{\perp 2}(x, y, \xi) = \lambda \hat{W}_{\perp 2}(\xi)[\langle x^2 - y^2 \rangle(x\hat{x} - y\hat{y}) \\ + \langle 2xy \rangle(y\hat{x} + x\hat{y})]. \tag{3}$$

The above expressions describe the linear transverse wake functions in the zeroth, first, and second order, respectively, where λ is the beam charge per unit length, the angle bracket is the average of particles at a given slice, $\hat{W}_{\perp m}(\xi)(m = 0, 1, 2...)$ are coefficients determined by the parameters of hollow channel [15], and $\xi \equiv ct - z$. The overall wake function is the summation of all modes, but usually these low-order terms suffice. The electromagnetic field is the convolution of wake function and charge distribution along ξ. For practical finite-thickness plasma channel, these equations are still useful approximations [24].

Inside the hollow channel, the transverse wakefield vanishes to the zeroth order, and other terms depend on the beam distribution. An on-axis axisymmetric bunch can propagate in the channel without any deflecting force. But if it is misaligned, the corresponding dipole wakefield as indicated by Eq. (2) deflects the beam toward the boundary. Instead, if the beam is transversely asymmetric with little offset, the quadrupole wakefield can be dominant and focus the beam in one plane and defocus it in the other until it reaches the plasma wall. In radio-frequency or dielectric accelerators, the high order wakefields have similar effects but must be suppressed or corrected [25,26] because once a particle hits the wall, it is lost. Since plasma is an ionized medium, the relativistic beam particles hitting the boundary repel the plasma electrons and expose the plasma ions. A stable equilibrium can then be found where the quadrupole defocusing forces are balanced by the Coulomb restoring force exerted by the ions, which ceases the deflection.

The evolution of an on-axis elliptical electron beam propagating in a hollow plasma channel is presented in Fig. 1. The QuickPic simulations used a $400 \times 400 \times 500 \ \mu m$ (x, y, ξ) simulation domain with $512 \times 512 \times 1024$ cells. The plasma has density $n_0 = 3.11 \times 10^{16} \ cm^{-3}$, inner and outer radii $50 \ \mu m$, $150 \ \mu m$, with skin depth $30 \ \mu m$. This beam has charge 2 nC, energy 5.11 GeV, tri-Gaussian profile with $\sigma_x = 20 \ \mu m$, $\sigma_y = 10 \ \mu m$, $\sigma_z = 30 \ \mu m$, and normalized emittances $\epsilon_{nx} = 20 \ \mu m \cdot rad$, $\epsilon_{ny} = 10 \ \mu m \cdot rad$. So $\langle x \rangle = \langle y \rangle = \langle xy \rangle = 0$ and $\langle x^2 - y^2 \rangle = \sigma_x^2 - \sigma_y^2$, and the leading term of transverse wake functions is $\vec{W}_{\perp 2} = \lambda \hat{W}_{\perp 2}(\xi)(\sigma_x^2 - \sigma_y^2)(x\hat{x} - y\hat{y})$, which defocuses the beam in x direction and focuses in y as plotted in Fig. 1(d). The beam gradually expands in x and compresses in y to increase its ellipticity. This drive beam is dense enough to evacuate the plasma electrons and expose the massive ions, but it does not punch through the channel wall. Instead, the Coulomb field of the exposed ions pulls it

back. This total internal guiding of the relativistic beam has been measured experimentally [27,28]. These electrons subsequently stay close to the plasma boundary while those inside the channel continue to move outward. Finally, after propagation of 10 cm, most drive beam electrons are trapped near the plasma boundary, forming a quasisteady state structure, as shown in Figs. 1(c),(f) and thereafter propagate stably. The drive beam eventually becomes equally divided into two parts.

The formation of the quasisteady state structure is robust as it occurs for other beams with asymmetric profiles in x and y. Larger degrees of asymmetry usually lead to stronger quadrupole wakefield and a shorter distance before a steady state is reached. Particularly, if the initial beam profile is close to the steady state profile, such as two bunches separated transversely, a stable state is obtained immediately once the beams enter the hollow plasma channel.

Transverse instability seeded by beam misalignment with respect to the channel axis is of major concern for hollow plasma channels. Here, we show that the asymmetric (elliptic) beam is far more stable against the beam-breakup instability than a round beam. Figure 2 illustrates the fully evolved (a) round and (b) elliptic beams and plasma profiles with initial centroid offset 0.1 μm in x direction. The round beam has $\sigma_r = 15$ μm, $\epsilon_{nr} = 15$ μm $\cdot$ rad, and other parameters the same as the above beam. The asymmetric beam is identical to that in Fig. 1. As aforementioned, a misaligned round beam excites a transverse wakefield dominated by a dipole mode, which kicks the beam toward the closest boundary. After propagation of 20 cm, this beam is totally deflected and hits the plasma wall. There is no place to load the witness e^+ bunch in this distorted plasma bucket. In contrast, the evolution of an asymmetric beam with some misalignment is quite similar to the on-axis situation. Figure 2(c) quantifies the evolvement of the beam centroid in x and y directions. For the symmetric beam, the centroid offset grows exponentially in the initial offset direction until most electrons are stopped at the plasma boundary. The mean offset $\langle x \rangle$ for the elliptic beam grows at the beginning but
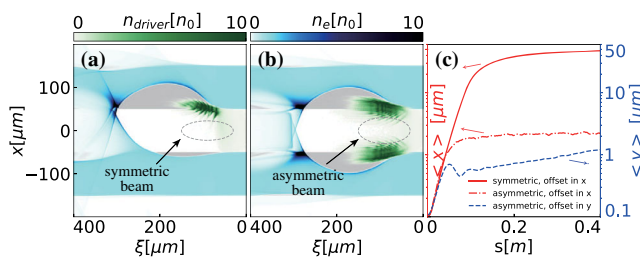
saturates at a much smaller extent ($\sim$2 μm). When the asymmetric beam has 0.1 μm offset in y direction, the evolution is qualitatively the same, but the beam drifts slowly in this direction. After 40 cm propagation, the centroid growth is about 1 μm. It may be possible to correct this offset using external magnets. Furthermore, asymmetric beams with other profiles can be explored to tolerate larger misalignments.

However, stable propagation of the driver does not ensure stable, efficient acceleration for e^+ beam. Guided e^+ transport and small emittance growth in plasma requires plasma electrons to flow through the positron bunch and provide a quasilinear focusing force. In fact, when the driver (100 pC e^- bunch with other parameters the same as in Fig. 1) is weak ($n_b < n_p$), it only slightly perturbs the plasma [Fig. 3(a)], and no plasma electrons are seen near the channel axis within the simulation box. The longitudinal field [Fig. 3(b)] is quasisinusoidal on axis reaching a peak value of 400 MV/m and nearly uniform in the transverse direction except near the slightly perturbed channel wall. The quadrupole wakefield dominates inside the channel [Figs. 3(c),(d)], which changes sign in y direction compared to the x direction, so e^+ cannot be confined in both planes when it is loaded at the accelerating phase right behind the drive beam. The situation is dramatically changed when the driver strength is strong enough to excite a half-blowout-like wake on the channel wall on either side, as shown in Fig. 3(e). In this 2 nC driver case, the longitudinal wakefield is an order of magnitude larger, is nonsinusoidal, reaches a peak value of about 8 GV/m, and is nearly independent of the transverse position inside the channel [Fig. 3(f)]. The returned plasma electrons that overshoot the channel boundary with some crossing the axis dominate the transverse wakefield structure inside the channel. As shown in Figs. 3(g),(h), there is now an approximately linear focusing force for positrons in

FIG. 2. (a),(b) Plasma and beam densities of a symmetric and asymmetric electron beam with initial offset 0.1 μm in x direction after 20 cm transportation in a hollow plasma channel. The dashed line is one-tenth of the maximum contour of the initial beam density. (c) The evolution of the average offset for the electron beams in x and y directions.
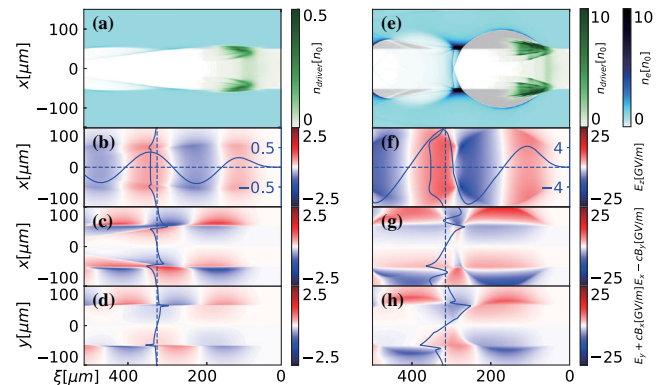

FIG. 3. Unloaded wakefields. (a)–(d) is of a 100 pC driver and (e)–(h) is of a 2 nC driver. (a),(e) Beam and plasma densities after stabilization. (b),(f) E_z field. Transverse wakefields in $x - \xi$ plane (c),(g) and $y - \xi$ plane (d),(h). The vertical lineouts of wakefields are at $\xi = 315$ μm.

both dimensions, offering the possibility of positron acceleration with mild emittance growth.

Also note that the transverse wakefield is quadrupole in the first bucket where the drive beam resides as expected. However, in about half-wavelength-long region coinciding with where the plasma electrons are observed inside the channel in Fig. 3(e) in the second bucket, the transverse wakefield is focusing for e^+ and has a similar magnitude in both transverse planes. This is the region [around the dash line at $\xi = 315$ μm in Figs. 3(f)–(h)] where fields are both accelerating and focusing that is suitable for beam-loaded e^+ acceleration.

Now we elaborate upon the physical effects seen in Fig. 3. For plasma electrons that are injected into the channel, the relationship between its transverse and longitudinal position is given by $dr/d\xi = v_r/(c - v_z)$, where v_r and v_z are the radial and longitudinal velocities, respectively. The wavelength of the longitudinal wakefield is roughly $\lambda_0 \sim 2\pi/k_p$ [15]. From Fig. 3, we find that at the beginning of the positive E_z those electrons are near the channel inner boundary. In order to load the positron beam at high gradient position, we desire $|\overline{dr/d\xi}| > r_0/(\lambda_0/4) = 2k_p r_0/\pi$. For parameters of the above channel, $2k_p r_0/\pi \sim 1.05$, which means the plasma electrons should be relativistic before entering into channel. This is normally satisfied when we are in the nonlinear regime of PWFA as in a uniform plasma with $\Lambda \sim 1$, where $\Lambda = \int_0^\infty k_p^2 r n_b/n_p dr$ is the normalized charge per unit length of the drive beam [5,29]. For the 2 nC and 100 pC drive beams, the peak Λ is 0.9 and 0.045, respectively, consistent with the analysis.

We then employ 3D particle-in-cell simulations using QuickPic to explore the positron beam-loading scenario. High efficiency positron acceleration inevitably involves strong interaction between positrons and plasma electrons, which will affect the wake to a great extent but in a complicated way. Surprisingly, we find that an intense e^+ beam does change the wakefield beneficially. Positrons attract plasma electrons inward and form an electron filament on the axis to augment the focusing force. Besides, when the positron beam is loaded at a proper phase, the longitudinal wakefield can be flattened, and high efficiency uniform acceleration is achieved.

The positron beam-loading effects once the 2 nC, 5.11 GeV elliptic driver bunch is stabilized are illustrated in Fig. 4. This e^+ beam contains 0.64 nC charge, initial energy 10.2 GeV, rms length 15 μm, and $\sigma_x = 5$ μm, $\sigma_y = 4$ μm, and the emittances $\epsilon_{nx} = 60$ μm, $\epsilon_{ny} = 50$ μm, that is close to the e^+ beam used in SLAC's FACET experiment [10]. The two beams were injected from the outside with a fixed separation of 225 μm. As in Figs. 4(a), (b), the majority of positrons are located at the focusing region and are confined, while a small fraction of the beam head is in the first bucket and gets deflected by the quadrupole transverse field. The deflection will cease when the
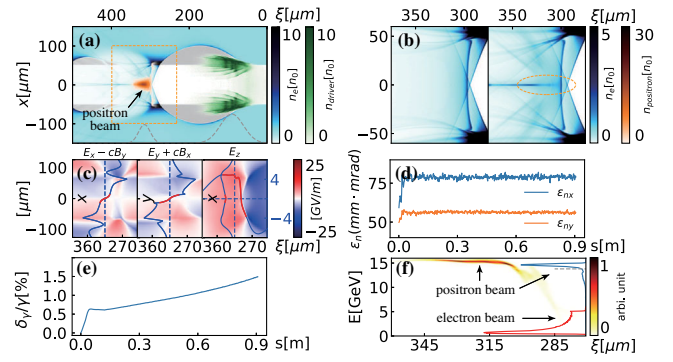

FIG. 4. Positron beam-loading effects. (a) Loaded plasma and beam densities, the gray dashed line is the current profile of two beams. (b) Plasma density in region of interest. Left: unloaded, right: beam-loading case. The dashed line is one-tenth of the maximum contour of the initial positron bunch density. (c) Loaded wakefields in the region denoted by the orange dashed line in (a). The red lines represent the range of $\pm 2\sigma_{x,z}$ for the positron beam. (d) Normalized slice emittance of the witness beam at $\xi = 315$ μm vs propagation distances. (e) Evolution of the energy spread of the witness beam with $\xi > 305$ μm. (f) Final energy spectra and longitudinal phase space of the witness beam, the dashed line represents energy of 13.8 GeV.

positrons arrive at the inner boundary and are refracted by the high density plasma electrons around the wall. So the beam charge is conserved during acceleration. An initially tailored current profile will help avoid this beam degradation. Figure 4(b) compares the plasma electron distribution inside the hollow channel for the unloaded and loaded cases. For the unloaded situation, these electrons nearly uniformly fill the cross section of the channel, while the intense transverse electric field of the e^+ beam confines some electrons to form an on-axis electron filament for the loaded situation. This filament has a smaller radius than the initial positron beam size and will vary with the e^+ beam profile and charge. Since the plasma electrons are not uniformly distributed in the transverse plane, the focusing field is no longer linear within the positron bunch and becomes stronger near the axis [Fig. 4(c)]. The evolution of the slice normalized emittance of the witness beam at beam center $\xi = 315$ μm is illustrated in Fig. 4(d). The emittance grows by 20% to 30% during the first 5 cm propagation when the drive beam evolves and stays constant for the rest. If the e^+ beam is injected after the driver is stabilized, the emittance growth should be strongly reduced. Previous study also finds that an overfocused beam can further reduce the emittance growth under this type of nonlinear focusing force [30].

The longitudinal wakefield shows the characteristic flattening due to beam-loading by the positron beam. These loaded positrons shape the profile of the E_z field by sucking in the returned plasma electrons and extract a substantial amount of energy from the wakefield. With a proper beam profile and loading phase, it is possible for the positron beam to get uniform acceleration. The E_z field in Fig. 4(c) confirms the flattening effect of the accelerating

field, with the peak value decreased from 8 GV/m to around 5 GV/m. At transverse direction, E_z is smaller near the axis because of the electron-positron interaction. Figure 4(e) plots the energy spread of the e^+ beam with $\xi > 305 \ \mu m$ (75% of the total charge) during acceleration. The energy spread increases from 0% to 0.7% after the first 5 cm, then slowly grows to about 1.5% during the next 85 cm. Final energy spectra are presented in Fig. 4(f). Some e^- almost deplete their energy, and most e^+ are accelerated to high energy while those in the front lose energy. The final longitudinal phase space shows a sharp chirp on the beam head and uniform acceleration for the rest, consistent with the E_z profile. For e^+ with $E > 13.8$ GeV, this part of the positrons contains 0.49 nC, and the mean energy is 14.6 GeV, corresponding to an average gradient of 4.9 GV/m with an rms energy spread of 1.6% and an energy transfer efficiency (the ratio of energy gained by this part to the energy transferred to the wake by the driver) of 33%.

In summary, we have demonstrated a viable scheme of efficient high-gradient acceleration of a positron bunch with a narrow energy spread using an electron beam to drive the wake in a hollow plasma channel. Moreover, this scheme appears very promising for further optimization through tailoring the beam profile, beam-loading phase, transverse size, and emittance, etc., to significantly improve the final beam quality and energy transfer efficiency.

---

[*]Corresponding author.
weilu@tsinghua.edu.cn

[1] X. Lou, Nat. Rev. Phys. **1**, 232 (2019).

[2] M. Benedikt, A. Blondel, P. Janot, M. Klein, M. Mangano, M. McCullough, V. Mertens, K. Oide, W. Riegler, D. Schulte, and F. Zimmermann, Annu. Rev. Nucl. Part. Sci. **69**, 389 (2019).

[3] P. Chen, J. M. Dawson, R. W. Huff, and T. Katsouleas, Phys. Rev. Lett. **54**, 693 (1985).

[4] J. B. Rosenzweig, Phys. Rev. Lett. **58**, 555 (1987).

[5] W. Lu, C. Huang, M. Zhou, W. B. Mori, and T. Katsouleas, Phys. Rev. Lett. **96**, 165002 (2006).

[6] M. Litos, E. Adli, W. An, C. I. Clarke, C. E. Clayton, S. Corde, J. P. Delahaye, R. J. England, A. S. Fisher, J. Frederico, S. Gessner et al., Nature (London) **515**, 92 (2014).

[7] C. Joshi, S. Corde, and W. B. Mori, Phys. Plasmas **27**, 070602 (2020).

[8] I. Blumenfeld, C. E. Clayton, F.-J. Decker, M. J. Hogan, C. Huang, R. Ischebeck, R. Iverson, C. Joshi et al., Nature (London) **445**, 741 (2007).

[9] B. E. Blue, C. E. Clayton, C. L. O'Connell, F. J. Decker, M. J. Hogan, C. Huang, R. Iverson, C. Joshi, T. C. Katsouleas et al., Phys. Rev. Lett. **90**, 214801 (2003).

[10] S. Corde, E. Adli, J. M. Allen, W. An, C. I. Clarke, C. E. Clayton, J. P. Delahaye, J. Frederico, S. Gessner, S. Z. Green et al., Nature (London) **524**, 442 (2015).

[11] A. Doche, C. Beekman, S. Corde, J. M. Allen, C. I. Clarke, J. Frederico, S. J. Gessner, S. Z. Green, M. J. Hogan et al., Sci. Rep. **7**, 14180 (2017).

[12] E. Adli, A. Ahuja, O. Apsimon, R. Apsimon, A. M. Bachmann, D. Barrientos, F. Batsch, J. Bauche, V. K. Berglyd Olsen, M. Bernardini et al., Nature (London) **561**, 363 (2018).

[13] T. C. Chiou, T. Katsouleas, C. Decker, W. B. Mori, J. S. Wurtele, G. Shvets, and J. J. Su, Phys. Plasmas **2**, 310 (1995).

[14] T. C. Chiou and T. Katsouleas, Phys. Rev. Lett. **81**, 3411 (1998).

[15] C. B. Schroeder, D. H. Whittum, and J. S. Wurtele, Phys. Rev. Lett. **82**, 1177 (1999).

[16] C. B. Schroeder, C. Benedetti, E. Esarey, and W. P. Leemans, Phys. Plasmas **20**, 123115 (2013).

[17] S. Gessner, E. Adli, J. M. Allen, W. An, C. I. Clarke, C. E. Clayton, S. Corde, J. P. Delahaye, J. Frederico et al., Nat. Commun. **7**, 11785 (2016).

[18] C. A. Lindstrøm, E. Adli, J. M. Allen, W. An, C. Beekman, C. I. Clarke, C. E. Clayton, S. Corde, A. Doche, J. Frederico et al., Phys. Rev. Lett. **120**, 124802 (2018).

[19] N. Jain, T. M. Antonsen, and J. P. Palastro, Phys. Rev. Lett. **115**, 195001 (2015).

[20] S. Diederichs, T. J. Mehrling, C. Benedetti, C. B. Schroeder, A. Knetsch, E. Esarey, and J. Osterhoff, Phys. Rev. Accel. Beams **22**, 081301 (2019).

[21] A. A. Sahai, arXiv:1610.03289.

[22] C. Huang, V. Decyk, C. Ren, M. Zhou, W. Lu, W. Mori, J. Cooley, T. Antonsen, and T. Katsouleas, J. Comput. Phys. **217**, 658 (2006).

[23] W. An, V. K. Decyk, W. B. Mori, and T. M. Antonsen, J. Comput. Phys. **250**, 165 (2013).

[24] S. J. Gessner, Ph.D. thesis, Stanford University, 2016.

[25] V. Balakin, A. Novohatsky, and V. Smirnov, in *12th International Conference on High-Energy Accelerators, HEACC 1983: Fermilab, Batavia, 1983* (1983), pp. 119–120.

[26] B. D. O'Shea, G. Andonian, S. S. Baturin, C. I. Clarke, P. D. Hoang, M. J. Hogan, B. Naranjo, O. B. Williams, V. Yakimenko, and J. B. Rosenzweig, Phys. Rev. Lett. **124**, 104801 (2020).

[27] P. Muggli, S. Lee, T. Katsouleas, R. Assmann, F.-J. Decker, M. J. Hogan, R. Iverson, P. Raimondi et al., Nature (London) **411**, 43 (2001).

[28] P. Muggli, S. Lee, T. Katsouleas, R. Assmann, F. J. Decker, M. J. Hogan, R. Iverson, P. Raimondi, R. H. Siemann, D. Walz, B. Blue, C. E. Clayton, E. Dodd, R. A. Fonseca, R. Hemker, C. Joshi, K. A. Marsh, W. B. Mori, and S. Wang, Phys. Rev. ST Accel. Beams **4**, 091301 (2001).

[29] W. Lu, C. Huang, M. Zhou, M. Tzoufras, F. S. Tsung, W. B. Mori, and T. Katsouleas, Phys. Plasmas **13**, 056709 (2006).

[30] W. An, W. Lu, C. Huang, X. Xu, M. J. Hogan, C. Joshi, and W. B. Mori, Phys. Rev. Lett. **118**, 244801 (2017).